Regulatory Toxicology and Pharmacology 58 (2010) 121–130

Contents lists available at ScienceDirect

Regulatory Toxicology and Pharmacology

journal homepage: www.elsevier.com/locate/yrtph

Suppressive effect of astaxanthin on retinal injury induced by elevated intraocular pressure

Aysegul Cort [a], Nihal Ozturk [d], Deniz Akpinar [d], Mustafa Unal [b], Gultekin Yucel [a], Akif Ciftcioglu [c], Piraye Yargicoglu [d], Mutay Aslan [a,*]

[a] Department of Biochemistry, Akdeniz University, School of Medicine. Antalya 07070, Turkey
[b] Department of Ophthalmology, Akdeniz University, School of Medicine. Antalya 07070, Turkey
[c] Department of Pathology, Akdeniz University, School of Medicine. Antalya 07070, Turkey
[d] Department of Biophysics, Akdeniz University, School of Medicine. Antalya 07070, Turkey

ARTICLE INFO

Article history:
Received 29 January 2010
Available online 8 May 2010

Keywords:
Astaxanthin
Intraocular pressure
Visual evoked potentials
Apoptosis

ABSTRACT

The aim of this study was to clarify the possible protective effect of astaxanthin (ASX) on the retina in rats with elevated intraocular pressure (EIOP). Rats were randomly divided into two groups which received olive oil or 5 mg/kg/day ASX for a period of 8 weeks. Elevated intraocular pressure was induced by unilaterally cauterizing three episcleral vessels and the unoperated eye served as control. At the end of the experimental period, neuroprotective effect of ASX was determined via electrophysiological measurements of visual evoked potentials (VEP) and rats were subsequently sacrificed to obtain enucleated globes which were divided into four groups including control, ASX treated, EIOP, EIOP + ASX treated. Retinoprotective properties of ASX were determined by evaluating retinal apoptosis, protein carbonyl levels and nitric oxide synthase-2 (NOS-2) expression. Latencies of all VEP components were significantly prolonged in EIOP and returned to control levels following ASX administration. When compared to controls, EIOP significantly increased retinal protein oxidation which returned to baseline levels in ASX treated EIOP group. NOS-2 expression determined by Western blot analysis and immunohistochemical staining was significantly greater in rats with EIOP compared to ASX and control groups. Retinal TUNEL staining showed apoptosis in all EIOP groups; however ASX treatment significantly decreased the percent of apoptotic cells when compared to non treated ocular hypertensive controls. The presented data confirm the role of oxidative injury in EIOP and highlight the protective effect of ASX in ocular hypertension.

1. Introduction

Experimental studies of induced ocular pressure elevation in nonhuman primates result in typical optic nerve damage as observed in glaucoma (Gaasterland et al., 1978; Quigley and Addicks, 1980). Glaucoma is a progressive optic neuropathy characterized by nerve fiber layer damage and is the second leading cause of blindness worldwide (Quigley, 1996). Glaucoma can occur in all age groups, including in infants, but it is most common in elderly people (Quigley, 1996). The pathophysiological mechanisms leading to optic neuropathy in glaucoma remain uncertain and the debate continues about whether damage to the optic nerve is caused by mechanical compression via elevated eye pressure or vascular ischemia leading to decreased blood flow to the optic nerve head. Irrespective of what causes the damage, the end result is progressive degeneration of retinal ganglion cells (RGCs) and their axons leading to glaucomatous optic neuropathy (GON) (Coleman, 1999). The most common types of glaucoma are primary open-angle glaucoma (POAG) and primary angle-closure glaucoma (PACG) which are both characterized by damage to the optic nerve and visual field loss (Coleman, 1999). These types of glaucoma can be determined by the mechanism of elevated intraocular pressure (IOP). Impaired outflow of aqueous humor resulting from abnormalities within the drainage system of the anterior chamber angle can cause open-angle glaucoma, while impaired access of aqueous humor to the drainage system results in angle-closure glaucoma (Salmon, 2008).

The mechanical compression theory explaining the origin of glaucoma considers elevated IOP as the most important risk factor for the disease (Yan et al., 1994). This theory gives support to the essential signs of glaucomatous optic neuropathy, such as increased cupping and neuroretinal rim thinning (Jonas et al., 1998) but does not explain the existence of normal tension glaucoma (Ishida et al., 1998). Alternatively, the vascular ischemia theory supposes that vascular insufficiency in the optic nerve head results in decreased metabolic activity which subsequently leads

* Corresponding author. Address: Akdeniz University Medical School, Department of Biochemistry, 07070 Antalya, Turkey. Fax: +90 242 2274482.
E-mail address: mutayaslan@akdeniz.edu.tr (M. Aslan).

0273-2300/$ - see front matter © 2010 Elsevier Inc. All rights reserved.
doi:10.1016/j.yrtph.2010.05.001

to increased glutamate accumulation and ganglion cell death (Sucher et al., 1997). Indeed, a large number of studies have shown a high association between glaucomatous optic neuropathy and vascular disorders related to hypertension, diabetes and hypercholesterolemia (Nemesure et al., 2003).

Oxidative stress has been implicated to cause increased IOP by triggering trabecular meshwork (TM) degeneration and thus contributing to alterations in the aqueous outflow pathway (Saccà et al., 2007). Indeed, treatment with hydrogen peroxide (H_2O_2) impairs trabecular meshwork cell adhesion to the extracellular matrix and causes rearrangement of cytoskeletal structures (Zhou et al., 1999). Trabecular meshwork cells show reduced sensitivity to H_2O_2 when cells are treated with timolol (Miyamoto et al., 2009), a non-selective beta-adrenoceptor antagonist currently used as an ocular preparation for the treatment of glaucoma (Nieminen et al., 2007). Timolol has been shown to induce the expression of peroxiredoxin-2 (Miyamoto et al., 2009), which functions as an antioxidant enzyme such as catalase and glutathione-dependent peroxidase (Hall et al., 2009). It has also been demonstrated that oxidative DNA damage is significantly greater in TM cells of glaucoma patients compared to controls (Izzotti, 2003). Moreover, in vivo studies in humans have shown that both IOP increase and visual field damage are significantly related to the amount of oxidative DNA damage (Saccà et al., 2005). Similarly, severity of optic nerve damage in eyes with primary open-angle glaucoma is correlated with changes in the TM (Gottanka et al., 1997).

Retinal oxidative injury occurring in models of elevated intraocular pressure or in normal tension glaucoma also directly damage the retinal ganglion cell layer, leading to GON (Tezel, 2006). Free radical injury has been reported to cause caspase independent cell death in RGCs *in vitro*. (Tezel and Yang, 2004). Furthermore, many retinal proteins exhibit oxidative modifications in experimental glaucoma, which may lead to important structural and functional alterations (Tezel et al., 2005).

Ocular tissues and fluids contain antioxidants that play a key role in protecting against oxidative damage. However, specific activity of a major antioxidant enzyme, superoxide dismutase (SOD), demonstrates an age-dependent decline in normal human trabecular meshwork (De La Paz and Epstein, 1996). Similarly, plasma glutathione levels assessed in 21 patients with newly diagnosed primary open-angle glaucoma and 34 age- and gender-matched control subjects revealed that glaucoma patients exhibited significantly lower levels of reduced and total glutathione than did control subjects (Gherghel et al., 2005).

A recent study performed on cultured retinal ganglion cells showed that astaxanthin (ASX), a naturally occurring carotenoid pigment and a powerful biological antioxidant (Palozza and Krinsky, 1992) inhibited the neurotoxicity induced by H_2O_2 or serum deprivation and reduced intracellular oxidation induced by various reactive oxygen species (Nakajima et al., 2008). Astaxanthin has a molecular structure similar to that of β-carotene (Fig. 1). However, it has thirteen conjugated double bonds, in contrast to eleven in β-carotene, which gives it significantly greater antioxidant capacity (Shibata et al., 2001). Moreover, ASX has hydroxyl groups in the 3 and 3′ positions, making the molecule highly polar and dramatically enhances its ability to cross the blood brain barrier of the retinal pigment epithelium and protect against degenerative conditions (Shibata et al., 2001). Astaxanthin stabilizes free radicals by adding them to its long double-bond chain rather than donating an atom or electron to the radical. Consequently, it can resist chain reactions that occur when a fatty acid is oxidized, thus allowing it to scavenge or quench longer than antioxidants that cannot stop this chain reaction (Kurashige et al., 1990). In-vivo studies in mice have also demonstrated that astaxanthin reduces retinal damage induced by intravitreal *N*-methyl-D-aspartate (NMDA) injection (Nakajima et al., 2008). Based on the role of reactive oxygen and nitrogen species in the pathogenesis of glaucoma (Aslan et al., 2008) and the relevance of ASX protection against retinal neurodegeneration, this study aimed to examine the effect of ASX treatment in rats with increased intraocular pressure.

2. Materials and methods

2.1. Animals

All experimental protocols conducted on rats were performed in accordance with the standards established by the Institutional Animal Care and Use Committee at Akdeniz University Medical School. Male Wistar rats weighing 350–450 g were housed in stainless steel cages and given food and water ad libitum. Animals were maintained at 12 h light–dark cycles and a constant temperature of 23 ± 1 °C at all times. The illumination in the room the animals were housed ranged from approximately 100 lux (bottom shelf of the animal rack) to 300 lux (top shelf of the animal rack) during the light cycle. All rats included in the study were kept in cages that were placed on the bottom shelf of the animal rack. Rats were randomly divided into two groups of 20 animals each which received olive oil or 5 mg/kg/day ASX (3,3-dihydroxybeta,beta-carotene-4,4-dione; Sigma–Aldrich Chemie, Steinheim, Germany) dissolved in olive oil via oral gavage for a period of 8 weeks. Astaxanthin treatment was initiated on the day the animals were operated.

2.2. Rat model of elevated intraocular pressure

Intraocular pressure was elevated in rats by cauterizing three episcleral vessels, as previously described (Sawada and Neufeld, 1999; Shareef et al., 1995). Briefly, rats were anesthetized intraperitoneally with a mixture of ketamine (25 mg/kg, Richter Pharma AG, Wels, Austria) and xylazine hydrochloride (5 mg/kg, Alfasan International B.V., Woerden, Holland). Episcleral vessels were exposed by incising the overlying conjunctiva and cauterized via an ophthalmic cautery. Pain relief was provided to all rats via intramuscular (im) injections of tramadol hydrochloride (2 mg/kg; CONTRAMAL, Abdi Ibrahim, Istanbul, Turkey), given twice with 12-h intervals, following the first day of post-operative treatment. Intraocular pressure was measured before surgery and every week after surgery over a 2-month period. A handheld tonometer (XL-Tonopen, Mentor O and O, Norwell, MA, USA) was used to measure IOP in rats under ether anesthesia. It has previously been reported that all anesthetics result in significant reduction in measured IOP when compared with the corresponding awake IOP (Jia et al., 2000). However, it was not

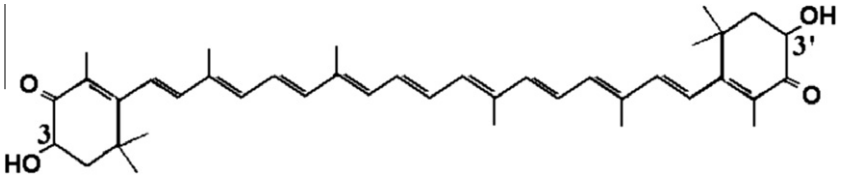

Fig. 1. Structure of astaxanthin (3,3′-dihydroxybeta, beta-carotene-4,4-dione).

possible to do the measurements on awake animals. Intraocular pressure measurements were performed as described in the instruction manual of the tonometer. The mean IOP of 5–10 consecutive measurements were recorded. Operated eyes served as EIOP while the unoperated eyes were control. At the end of the 8 week experimental period, visual evoked potentials were recorded between 10.00 AM and 2.00 PM and animals were sacrificed the next day under anesthesia by exsanguination via cardiac puncture. Enucleated globes were divided into four groups of 20 eyes each as follows; control, ASX treated, EIOP and EIOP + ASX treated.

2.3. Visual evoked potential recordings

Visual evoked potentials were recorded between 10.00 AM and 2.00 PM and animals were sacrificed the next day at the same time interval. Visual evoked potentials were recorded with stainless steel subdermal electrodes (Nihon Kohden NE 223 S, Nihon Kohden Corporation, Tokyo 161, Japan) under ether anesthesia as previously described (Akpinar et al., 2007). The reference and active electrodes were placed 0.5 cm in front of and behind bregma, respectively. The active electrode was also placed 0.4 cm lateral to the midline over area 17 of visual cortex. A ground electrode was placed on the tails of animals. After 5 min of dark adaptation, a photic stimulator (Nova-Strobe AB, Biopac System Inc., Santa Barbara, CA 93117, USA) at the lowest intensity setting was used to provide the flash stimulus at a distance of 15 cm, which allowed lighting of the entire pupilla from the temporal visual field. Repetition rate of flash stimulus was 1 Hz and flash energy was 0.1 J. VEP recordings from both right and left were obtained, and throughout the experiments the eye not under investigation was occluded by appropriate black carbon paper and cotton. Body temperature was maintained between 37.5 and 38 °C via a heating pad and monitored with a rectal thermometer probe (Havard Apparatus Homoeothermic Blanket Control Unit, Havard Apparatus Ltd. Kent, United Kingdom).

The averaging of 100 responses was accomplished with the averager of Biopac MP100 data acquisition equipment (Biopac System Inc., Santa Barbara, CA 93117, USA). Analysis time was 300 ms. The frequency bandwidth of the amplifier was 1–100 Hz. The gain was selected 20 μV/div. The sampling rate of the VEP recording was 2000 samples. The microprocessor was programmed to reject any sweeps contaminated with larger artifacts, and at least two averages were obtained to ensure response reproducibility. Peak latencies of the components were measured from the stimulus artifact to the peak in milliseconds. Amplitudes were measured as the voltage between successive peaks. Measurements were made on three positive and two negative potentials which are seen in all groups.

2.4. Immunohistochemical staining

Enucleated globe materials were fixed in 10% buffered formalin solutions and incised in transverse plain just from the center of the globe to obtain two equal parts. Fixed tissues were washed in phosphate buffered saline (pH 7.4), embedded in paraffin and cut into 4-μm sections. For peroxidase staining, sections were deparaffined, rehydrated and washed with Tris buffered saline. Endogenous peroxidase activity was blocked by incubating tissue sections with 3% hydrogen peroxide for five minutes prior to application of the primary antibody. Primary antibody incubations were at 25 °C for 60 min using rabbit polyclonal anti-NOS2 (1:100 dilution, Santa Cruz Biotechnology, Santa Cruz, CA). After sections were washed they were immunostained with an avidin–biotin complex kit (Dako, Carpinteria, CA) followed by hematoxylin counterstaining. Negative controls were performed by replacing the primary antibody with nonimmune serum followed by immunoperoxidase staining. Presence of a red-brown colored end-product in the cytoplasm was indicative of positive staining. Counterstaining with hematoxylin resulted in a pale to dark blue coloration of cell nuclei. All stained tissue sections were visualized via light microscopy (Olympus IX81, Tokyo, Japan).

To obtain a quantitative standard for NOS-2 immunostaining within the different experimental groups morphometric analysis was performed as previously described (Yücel et al., 2005). The immunostaining scores, obtained according to both the percentage and intensity of positive stained cells, were statistically analyzed by Sigma Stat (version 2.03) software for windows. The percentage of the positive stained cells was scored as follows: 0 = less than 5% of the cells/high powered field (HPF, 40·) are stained, 1 = 5% to less than 30% of cells/HPF are stained. 2 = 30% to less than 50% of cells/HPF are stained. 3 = more than 50% of cells/HPF are stained. The intensity of staining within each counted cell was also scored as follows: 0 = no staining, 1 = weak staining (pale red–brown), 2 = moderate staining (red–brown), 3 = strong staining (dark red–brown). A final immunostaining score was obtained for all sections by adding the two scores.

2.5. TUNEL analysis

Apoptotic cells were visualized with the terminal deoxynucleotide transferase (TdT) FragEL DNA fragmentation kit (Oncogene, Boston, MA) analogous to TdT mediated nick endlabeling. Dark brown cells with pyknotic nuclei were indicative of positive staining for apoptosis, whereas green to greenish color signified a nonreactive cell. To obtain a quantitative standard for apoptotic cell death within the different experimental group's morphometric analysis was performed on all retinal sections by a pathologist blinded to the experimental conditions.

2.6. SDS–PAGE and Western blot analysis

Retina was harvested from enucleated globes and homogenized in 2 ml ice-cold homogenizing buffer (50 mM K_2HPO_4, 80 μM leupeptin (Sigma–Aldrich, Steinheim, Germany), 2.1 mM Pefabloc SC (SERVA, Heidelberg, Germany), 1 mM phenylmethylsulfonyl fluoride (Sigma–Aldrich), 1 μg/ml aprotinin (SERVA; pH 7.4). Homogenates were centrifuged (40,000g, 30 min, 4 °C) and supernatants were stored at −80 °C until analyzed. For Western blot analysis, tissue proteins were separated by SDS–PAGE and transferred to nitrocellulose membranes. A rabbit polyclonal antibody against NOS-2 (1:800 dilution; BD Transduction Laboratories, San Jose, CA) was used for immunoblot analysis. Horseradish peroxidase–conjugated goat anti-rabbit IgG (1:10,000 dilution; Zymed Laboratories, San Francisco, CA) was used as a secondary antibody, and immunoreactive proteins were visualized by chemiluminescence via ECL reagent (Amersham Pharmacia Biotech, Buckinghamshire, England). Proteins separated by SDS–PAGE were also visualized by Electro-Blue Staining solution (Qbiogene, Heidelberg, Germany).

2.7. Measurement of tissue GSH and GSSG content

Glutathione (GSH) and glutathione disulfide (GSSG) levels were measured by a commercially available GSH assay kit (Cat. #703002. Cayman Chemical Ann Arbor, MI). Retina harvested from enucleated globes were homogenized in ice-cold phosphate buffer (50 mM K_2HPO_4, containing 1 mM EDTA, pH 7). Homogenates were centrifuged (10,000g, 15 min, 4 °C) and supernatants were deproteinated in 10% metaphosphoric acid (Sigma Aldrich, Steinheim, Switzerland). The GSSG was reduced to GSH by GSH reductase in the assay cocktail of the kit containing DTNB (5,5′-dithiobis-2-nitrobenzoic acid, Ellman's reagent), glucose-6-phosphate dehydrogenase, GSH reductase, $NADP^+$ and glucose-6-phosphate. The

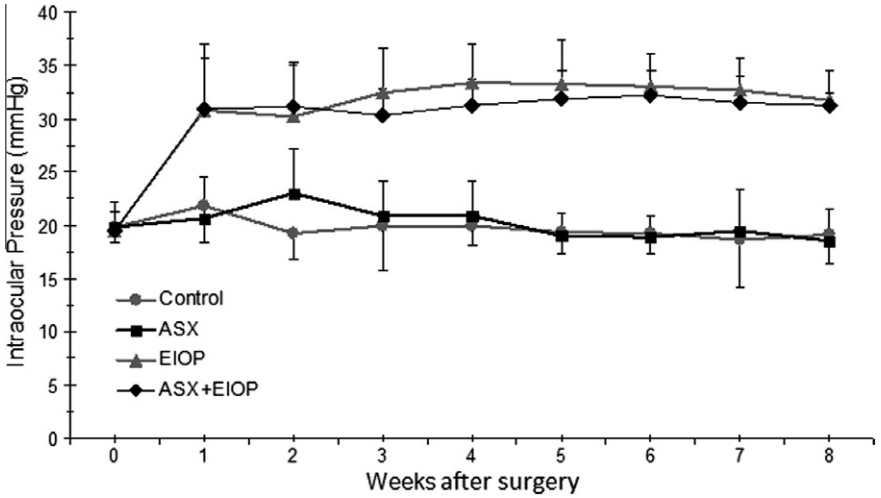

Fig. 2. Intraocular pressure measurements of eyes. ASX, astaxanthin; EIOP, elevated intraocular pressure. Values represent means ± SD.

sulfhydryl group of GSH reacts with DTNB to give a yellow colored 5-thio-2-nitrobenzoic acid (TNB) which is measured at an absorbance of 405 nm. Tissue levels of GSSG were determined by first derivatizing GSH with 2-vinylpyridine (Sigma Aldrich, Steinheim, Switzerland). The values of GSSG and total GSH for each sample were calculated from their respective slopes using a GSSG or GSH standard curve.

2.8. Measurement of tissue protein carbonyl content

Protein-bound carbonyls were measured via a protein carbonyl assay kit (Cat. #1005020 Cayman Chemical, Ann Arbor MI). The utilized method was based on the covalent reaction of the carbonylated protein side chain with 2,4 dinitrophenyl-hydrazine (DNPH) and detection of the produced protein-hydrazone at an absorbance of 370 nm. The results were calculated using the extinction coefficient of 22 $mM^{-1}\,cm^{-1}$ for aliphatic hydrazones and were expressed as nmol/mg protein.

2.9. Measurement of lipid peroxidation

Levels of MDA, a product of lipid peroxidation, was measured using the thiobarbituric acid (TBA) fluorometric assay (Wasowicz et al., 1993) with 1,1,3,3-teraethoxypropane as a standard. Briefly, 50 μl of tissue sample was added to 1 ml distilled water which was then mixed with equal volumes of 29 mM TBA in acetic acid. After 1 h incubation at >95 °C, samples were cooled and 25 μl of 5 mM HCl was added. The final reaction mixture was extracted with 3.5 ml of *n*-butanol and the butanol phase was separated via centrifugation at 1500*g* for 5 min. MDA levels were determined fluorometrically (Perkin Elmer LS-45, Waltham, MA) with excitation and emission wavelengths of 532 nm and 547 nm, respectively. Protein concentrations were measured at 595 nm by a modified Bradford assay using Coomassie Plus reagent with bovine serum albumin as a standard (Pierce Chemical Company, Rockford, IL).

3. Results

3.1. Intraocular pressure levels

Intraocular pressure of eyes in which three aqueous vessels were cauterized is represented as EIOP, and is compared to the controlateral eyes. Intraocular pressure (mean ± SD) measured in non-cauterized eyes were 19.67 ± 0.90 and 20.12 ± 1.40 mm Hg for control ($n = 20$) and ASX treated ($n = 20$) groups, respectively. An increase of about 10 mm Hg was observed in cauterized eyes compared to respective controls with values of 30.78 ± 1.19 mm Hg in EIOP ($n = 20$) and 30.01 ± 0.58 mm Hg in ASX + EIOP ($n = 20$). Recorded IOP from cauterized eyes remained elevated over the 2 months experimental period (Fig. 2).

3.2. Retinal protein carbonyl and lipid peroxidation levels

Protein carbonyl levels were significantly increased in EIOP when compared to control ($p < 0.01$), ASX ($p < 0.01$) and ASX + EIOP groups ($p < 0.01$). Treatment with ASX significantly reduced levels of protein carbonyl formation in eyes with EIOP (Table 1). No significant difference was observed in protein carbonyl levels measured in ASX treated eyes alone when compared to control and

Table 1
Retina protein carbonyl, GSH, GSSG and MDA content. ASX, astaxanthin; EIOP, elevated intraocular pressure. The given values are means ± SD. Statistical analysis was by One Way Analysis of Variance with all pairwise multiple comparison procedures (Tukey Test). $^{*}p < 0.01$ compared to control and ASX. $^{**}p < 0.01$ compared to EIOP. $^{\#}p < 0.01$ compared to control, ASX and ASX + EIOP.

	Protein carbonyl (nmol/mg protein, $n = 12$)	GSH (nmol/mg protein, $n = 8$)	GSSG (nmol/mg protein, $n = 8$)	GSH:GSSG ($n = 8$)	MDA (nmol/g protein, $n = 12$)
Control	3.43 ± 1.75	2.64 ± 0.84	0.58 ± 0.06	4.59 ± 1.46	0.72 ± 0.14
ASX	5.17 ± 1.72	2.65 ± 0.4	0.57 ± 0.04	4.69 ± 0.8	0.56 ± 0.12
EIOP	7.9 ± 2.4*	1.95 ± 0.72	0.59 ± 0.12	3.31 ± 1.02	1.64 ± 0.43#
ASX + EIOP	3.6 ± 1.86**	2.25 ± 0.72	0.52 ± 0.16	4.43 ± 1.81	0.79 ± 0.16

ASX, astaxanthin; EIOP, elevated intraocular pressure. The given values are means ± SD. Statistical analysis was by One Way Analysis of Variance with all pairwise multiple comparison procedures (Tukey Test).
* $p < 0.01$ compared to control and ASX.
** $p = 0.007$ compared to EIOP.
# $p < 0.01$ compared to control, ASX and ASX + EIOP.

ASX + EIOP group. There was a significant increase ($p < 0.01$) in lipid peroxidation measured in rats with EIOP. Treatment of EIOP group with ASX decreased lipid peroxidation back to control levels (Table 1).

3.3. Retina glutathione, glutathione disulfide levels and GSH:GSSG ratios

Retina glutathione, glutathione disulfide levels and GSH:GSSG ratios are given in Table 1. No significant difference could be detected among the experimental groups. GSH:GSSG in the EIOP group was not significantly different from the others.

3.4. Nitric oxide synthase-2 expression

Fig. 3A demonstrates the localization of NOS-2 in retinal cross sections from representative rat in each of the four different groups. NOS-2 positive staining was observed throughout the outer plexiform layer (OPL), inner plexiform layer (IPL) and ganglion cell layer (GCL) in EIOP and ASX + EIOP groups. The photoreceptor cell layer (VCL) also showed diffuse NOS-2 immunostaining in EIOP and ASX + EIOP group rats. NOS-2 was not evident in eyes of control and ASX treated groups. The immunostaining scores, obtained according to both the percentage and intensity of positive stained cells were statistically increased in EIOP and ASX + EIOP group rats compared to control and ASX groups (Fig. 3B). Western blot analysis of retinal extracts using an anti-NOS2 antibody confirmed the observed immunostaining and revealed an immunodetectable 130 kDa protein band present only in EIOP and ASX + EIOP groups (Fig. 3C). Fig. 3D is Coomassie based staining of tissue proteins that were separated for Western blot analysis and shows equal protein loading in each lane.

3.5. Apoptosis

Fig. 4 shows representative photomicrographs of retinal TUNEL staining from each of the four groups. Apoptotic cells are seen in the GCL, outer and inner nuclear layers of all experimental groups. Percent of TUNEL-positive cells were significantly greater in both the ONL and INL of EIOP rat group when compared to all other experimental groups.

3.6. Visual evoked potentials

Representative waveforms of VEPs for all groups are presented in Fig. 5. Differences of VEP parameters were analyzed by ANOVA. The means and standard deviations of peak latencies of VEP components of all groups, and the results of the statistical analysis are shown in Table 2. The mean latencies of P1, N1, P2, N2 and P3 components were significantly prolonged in eyes with EIOP compared to control, ASX and ASX + EIOP groups ($p < 0.001$). Astaxanthin administration significantly ($p < 0.001$) decreased all VEP components in eyes with EIOP as compared to non treated eyes (Table 2). It was observed that there were no significant differences in amplitudes of VEP among experimental groups (Table 3).

4. Discussion

This study examined the effect of ASX treatment in retinal tissue injury resulting from elevated EIOP. Astaxanthin was dissolved in olive oil and administered at a dose of 5 mg/kg/day via oral gavage for a period of 8 weeks. Because carotenoids are lipid soluble, the amount and type of lipid with which they are consumed influence their absorption. The effect of different oils on the absorption of natural ASX, as used herein, was investigated in rats by continuously infusing 2.5–10 mg/ml of the compound into the duodenum. There was a significant linear relationship between the amount of ASX infused into the duodenum and the amount recovered in the lymph (Clark et al., 2000). Astaxanthin was more efficiently absorbed from olive oil than from corn oil emulsions. The efficiency of ASX absorption from olive oil averaged 20% with individual samples having a range of 14–28% (Clark et al., 2000). The oral bioavailability of natural ASX can be further supported by a study in which ASX content was measured in the liver, lung, kidney and small intestine of rats fed on 300 mg/kg ASX diet for 16 days (Jewell and O'Brien, 1999). The ASX content of liver, lung, kidney and small intestine of rats fed on ASX supplemented diet was 57.1 ± 6.6, 12.8 ± 0.2, 11.2 ± 0.3 and 209.5 ± 26.2 nmol/g tissue wet weight, respectively. Astaxanthin content was reported as 0.0 nmol/g tissue wet weight in the liver, lung, kidney and small intestine of rats fed on a control diet. A similar study was also conducted on rats to determine whether ASX had the ability to cross the blood-retinal brain barrier and concentrate in the retina. A dose of 150 mg of natural ASX, as used herein, was mixed with 1.5 ml of aqueous TWEEN-80 solution and injected intraperitoneally into six rats. After euthanizing the rats, the retinas were examined for the presence of ASX. After six consecutive intraperitoneal injections of ASX at 12 h intervals at a dose of 37.5 mg/kg of body weight, the average concentration of ASX in the retina was 170 ng/mg tissue wet weight after the last injection (Tso and Lam, 1996). It is of interest that in a more recent study, natural ASX accumulated in the eyes (80 ng/g tissue wet weight) after one week of 30 g/kg oral feed. Astaxanthin content was reported as 0.0 ng/g tissue wet weight in eyes of rats fed on a control diet (Petri and Lundebye, 2007). This is the same order of magnitude as was demonstrated for canthaxanthine in eyes of albino rats (130 ng/g wet weight) and pigmented rats (20 ng/g wet weight) after administration of 100 mg/kg feed for 5 weeks (JECFA, 1996).

The antioxidant effect of natural ASX in the eye was previously investigated in two different studies in rats. In the first study, light induced photoreceptor degeneration was conducted by exposing rats to 1800–2000 lux green filtered fluorescent light for 24 h after one day of total dark adaptation. A dose of 80 mg/kg/day of ASX in l ml of soybean oil were given to animals by daily oral feeding during the 2 week experimental period. A quantitative determination of photoreceptor cell injury, made by measuring the thickness of the outer nuclear layer, showed that ASX protected photoreceptor cells from photic injury (Tso and Lam, 1996). In the second study, the efficacy of ASX was investigated in lipopolysaccharide (LPS)-induced uveitis in rats. The rats were injected with 1, 10, or 100 mg/kg ASX before and after LPS administration. A dose of 1 mg/kg ASX significantly reduced nitrate/nitrite levels, TNF-alpha and prostaglandin E2, concentrations in the aqueous humor (Ohgami et al., 2003). Taking previously published data into consideration, we administered ASX at a dose of 5 mg/kg/day via oral gavage for a period of 8 weeks.

Mammals have limited ability to synthesize carotenoids de novo and thus rely upon diet to provide carotenoid requirements (Krinsky and Johnson, 2005). Ten carotenoids have been identified in human serum including beta-carotene, alpha-carotene, crptoxanthine, lycopene and lutein (Johnson, 2002). With the exception of beta-carotene, mammals are also incapable to modify carotenoids and thus deposit them unchanged in tissues (Stahl and Sies, 2005). Of the 10 carotenoids that have been reported in the human serum, only two, zeaxanthin and lutein are found in the human retina (Roberts et al., 2009). Although no strong association was observed between antioxidant consumption and the risk of primary open-angle glaucoma (Kang et al., 2003) it is suggested that zeaxanthin and lutein are concentrated in the retina because of their ability to cross the blood brain barrier of the retinal pigment epithelium and scavange free radicals (Landrum et al., 1999; Krinsky et al., 2003).

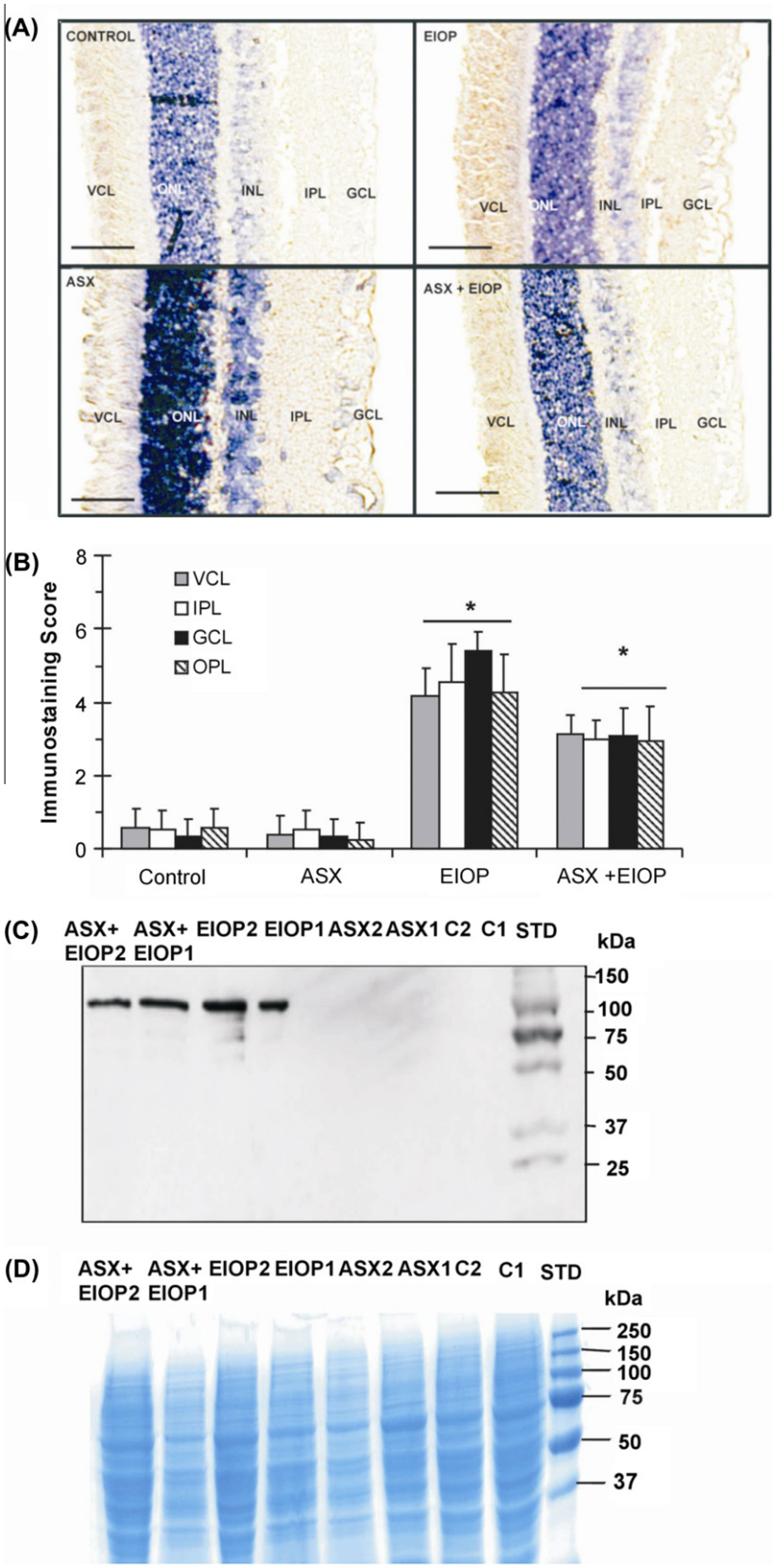

Fig. 3. (A) Immunostaining of NOS-2 in the retina. ASX, astaxanthin; EIOP, elevated intraocular pressure. Retinal photomicrographs of representative rat are shown from each of the four groups. GCL, ganglion cell layer; IPL, inner plexiform layer; INL, inner nuclear layer; ONL, outer nuclear layer; VCL, photoreceptor cell layer. Bars 200 μm. (B) Quantitation of NOS-2 in the retina. The immunostaining scores, obtained according to both the percentage and intensity of positive stained cells, were statistically analyzed by Sigma Stat (version 2.03) software for windows. Values represent means ± SD ($n = 6$). The differences in the immunostaining score among the different groups were analyzed via Kruskal–Wallis one way analysis of variance on ranks and all pairwise multiple comparisons were performed by Dunn's method. $^{*}p < 0.05$ compared to control and ASX. (C) Western blot analysis of NOS2. D) Coomassie blue staining of retinal proteins. C, control; ASX, astaxanthin; EIOP, elevated intraocular pressure.

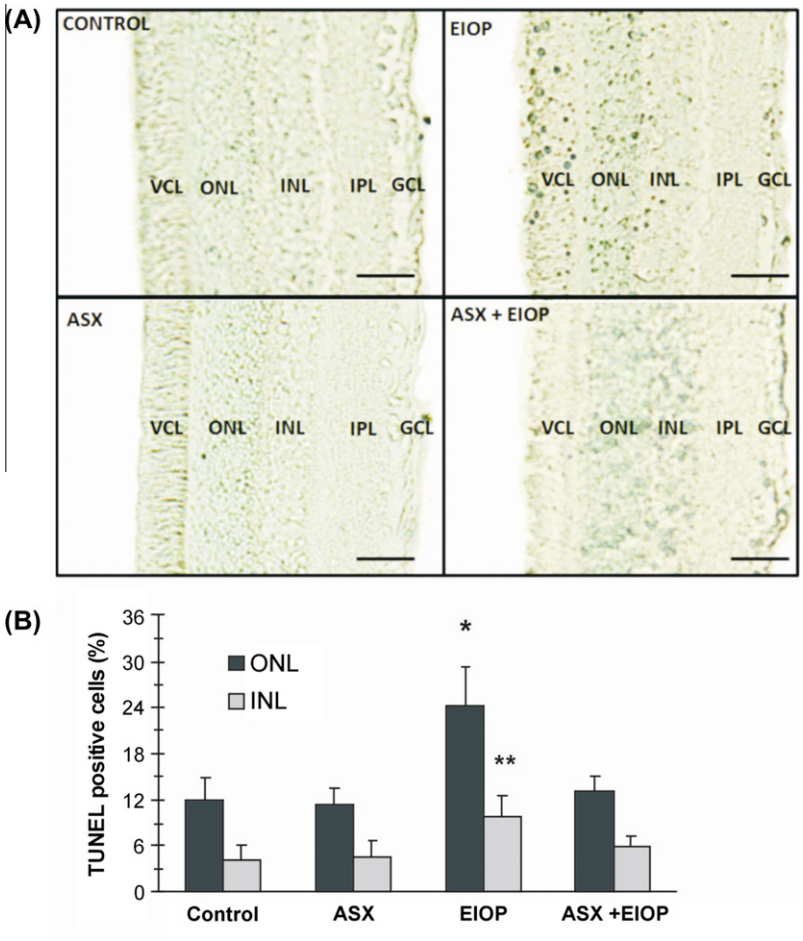

Fig. 4. A) TUNEL staining of the retina. GCL, ganglion cell layer; IPL, inner plexiform layer; INL, inner nuclear layer; ONL, outer nuclear layer; VCL, photoreceptor cell layer. ASX, astaxanthin; EIOP, elevated intraocular pressure. Bars 100 μm B) Percent of apoptotic cells in the retina. TUNEL-positive cells were quantified in the different layers of the retina. Cells present in five high powered fields (HPF, 40×) were counted in each section and the ratio of apoptotic cells was calculated as the percent of the whole cell number. Values are given as means ± SD ($n = 6$). Statistical analysis was performed by one way analysis of variance with all pairwise multiple comparison procedures done by Tukey test. $^{*}p < 0.001$ compared to ONL in control, ASX and ASX + EIOP groups. $^{**}p < 0.01$ compared to INL in control, ASX and ASX + EIOP groups.

To accomplish intraocular pressure elevation, episcleral vessels of the eye were cauterized as previously (Aslan et al., 2006) and an increase of about 10 mm Hg was observed in operated eyes following surgery which persisted over the 2-month experimental period. The measured increase in IOP compared well to previous levels reported in rats (Shareef et al., 1995; Cabrera et al., 1999).

Astaxanthin treatment significantly decreased protein carbonyl formation in the presence of intraocular pressure elevation (Table 1). Protein carbonyl formation is a widely utilized marker for protein oxidation (Stadtman and Oliver, 1991). Carbonyls, formed following reactive oxygen species-mediated oxidation of sugar and membrane lipids, are able to form adducts commonly known as CO-proteins (proteins bearing carbonyl groups) with structural proteins, causing alterations in their biological activity (Shacter, 2000). Reactive carbonyl groups on proteins can also be formed by direct oxidation of protein side-chains (Reznick and Packer, 1994). Reactive oxygen species may oxidize amino acid side-chains into ketone or aldehyde derivatives. As stated previously, ASX has a molecular structure similar to that of beta-carotene. However, it has thirteen conjugated double bonds in contrast to eleven in beta-carotene, which gives it significantly greater antioxidant capacity under systemic oxidant stress (Curek et al., 2010). Astaxanthin can scavange alkoxyl, hydroxyl, peroxyl radicals and inhibit the destruction of proteins caused by oxidation reactions (Naguib, 2000; Palozza and Krinsky, 1992).

The observed increase in NOS-2 protein (Figs. 3 and 4) is consistent with the involvement of NO cytotoxicity in EIOP (Shareef et al., 1999). Reported studies demonstrate the presence of NOS-2 in glaucomatous optic nerve heads with consistent staining of nitrotyrosine, indicating that reactive nitrogen species may contribute to retinal ganglion cell death associated with increased intraocular pressure (Liu and Neufeld, 2000; Shareef et al., 1999). Indeed, pharmacological studies have shown that inhibition of NOS-2 by aminoguanidine provides neuroprotection to retinal ganglion cells in a rat model of chronic glaucoma (Neufeld et al., 1999).

The major mechanism of visual loss in glaucoma is retinal ganglion cell apoptosis, leading to thinning of the inner nuclear and nerve fiber layers of the retina and axonal loss in the optic nerve (Fechtner and Weinreb, 1994). In animal models of ocular hypertension, elevated IOP augments apoptosis in retinal cells (Aslan et al., 2006) suggesting that nitrative stress exacerbates disease progression in clinical conditions accompanied by ocular degeneration (Aslan et al., 2007; Yücel et al., 2006).Ocular reactive oxygen and nitrogen species formation are important regulators of apoptosis which can be induced by two major pathways. The extrinsic pathway involves binding of TNF-α and Fas ligand to membrane receptors leading to caspase-8 activation, while the intrinsic pathway participates in stress-induced mitochondrial cytochrome *c* release (Aslan et al., 2008). The significant decrease in the percent of TUNEL-positive cells via ASX treatment (Fig. 4) further supports

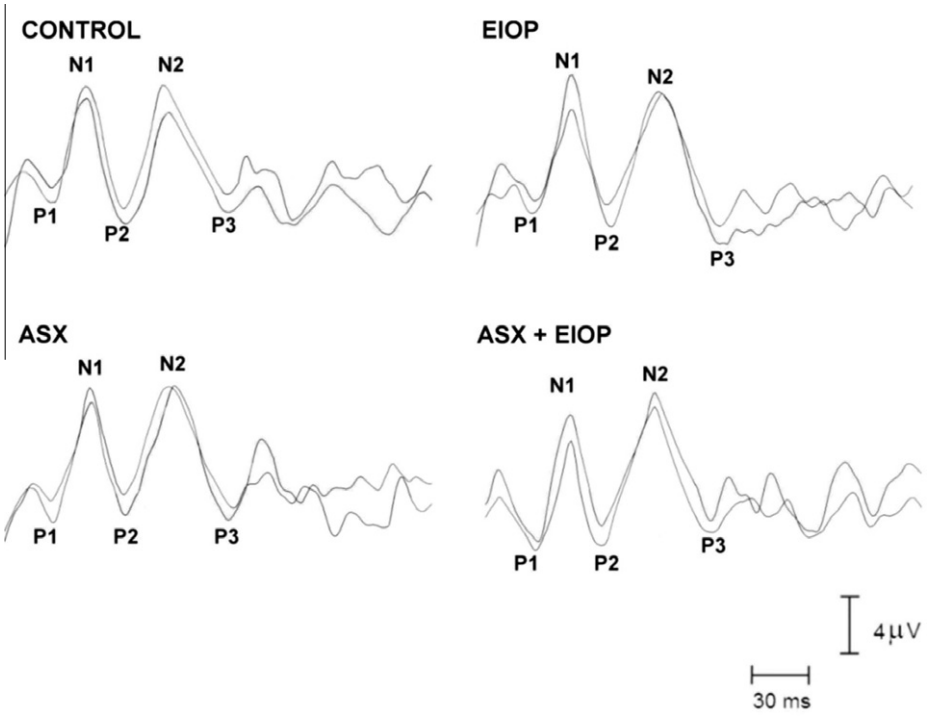

Fig. 5. Characteristic visual evoked potentials recorded from experimental groups. ASX, astaxanthin; EIOP, elevated intraocular pressure. Three positive (P1, P2, P3) and two negative (N1, N2) potentials were seen in all groups.

Table 2
The latencies for each VEP component.

Groups	P_1 (ms)	N_1 (ms)	P_2 (ms)	N_2 (ms)	P_3 (ms)
Control	20.17 ± 0.90	35.13 ± 1.96	50.40 ± 1.60	68.90 ± 2.84	94.47 ± 1.95
ASX	20.74 ± 0.85	36.47 ± 2.03	51.55 ± 2.65	71.03 ± 3.01	95.08 ± 2.21
EIOP	24.13 ± 1.06*	39.58 ± 1.41*	55.78 ± 2.04*	77.06 ± 1.17*	100.92 ± 1.2*
ASX + EIOP	20.73 ± 0.86	36.23 ± 1.60	51.14 ± 2.71	70.85 ± 3.77	93.69 ± 1.93

Values are means ± SD and $n = 10$.
* $p < 0.001$ compared to control, ASX and ASX + EIOP groups.

Table 3
The peak-to-peak amplitudes of each VEP component.

Groups	P1N1 (μV)	N1P2 (μV)	P2N2 (μV)	N2P3 (μV)
Control	5.86 ± 1.33	5.65 ± 1.75	5.51 ± 1.45	5.87 ± 1.55
ASX	6.26 ± 1.10	6.15 ± 1.44	5.30 ± 1.47	6.10 ± 1.45
EIOP	6.17 ± 1.57	5.89 ± 0.91	6.61 ± 1.66	6.04 ± 1.42
ASX + EIOP	6.27 ± 1.45	4.97 ± 1.20	6.27 ± 1.08	6.18 ± 1.33

Values are means ± SD and $n = 10$. No significant difference was observed in the recorded amplitudes among the different experimental groups.

the role of reactive oxygen species in apoptotic cell death and infers that deposition of ASX in the eye could provide superior protection against oxidant induced damage in retinal tissues.

The amplitudes and latencies of VEP components found in our laboratory are generally in agreement with those found in other laboratories (Silver et al., 1995). The present study showed that glaucoma resulted in prolongation of VEP latencies (Table 2). Considering that VEPs are a sensitive and reliable method to evaluate the earliest changes in the visual system (Lehman and Harrison, 2002), these results indicate that elevated IOP markedly affects the visual system. The changes in the initial portion of the VEP waveform suggest altered function in the "front end" of the visual system (Herr et al., 1995; Schroeder et al., 1991). The prolongation of late components (N2, P3) of VEPs may also reflect altered cortical processing of the visual stimulus (Herr et al., 1995). From our findings (Akpinar et al., 2007) together with previous results (Herr et al., 1995; Schroeder et al., 1991), it could be concluded that glaucoma-induced increase in VEP latencies may be due to delayed input to the visual cortex and/or alterations at the cortical level.

Prolonged latencies and no apparent difference in amplitudes observed in VEP components following intraocular pressure elevation (Tables 2 and 3) are in agreement with previous studies which have reported the presence of an abnormal VEP pattern in patients with ocular hypertension (OHT) (Howe and Mitchell, 1986; Towle et al., 1983). In OHT patients, delayed latencies have been recorded with preservation of amplitudes (Graham and Klistorner, 1998). Peroxidation damage has been shown to increase VEP latencies without altering the recorded amplitudes (Derin et al., 2009). In particular, oxidation of lipids found abundantly in cell membranes can lead to altered membrane structure and change neuronal functions (Bazan et al., 2005). This view is supported by presented results herein indicating that ASX treatment reduces electrophysiological alterations recorded via VEPs. This study is also the first to report that ASX treatment restores altered VEP parameters induced by elevated IOP.

Obtained results indicated that elevated IOP increased lipid peroxidation and prolonged VEP latencies. ASX treatment decreased

lipid peroxidation and VEP latencies of VEP components to control levels. Therefore, it could be concluded that lipid peroxidation might have a role in altered VEP responses in rats. Elevated IOP-induced lipid peroxidation observed in the retina is also in agreement with previous studies (Ko et al., 2005). Based on the reported data it is concluded that ASX treatment is beneficial in terms of reducing oxidant-induced protein oxidation, lipid peroxidation and apoptotic cell death in elevated IOP. This conclusion is supported by ASX's strong antioxidant activity, and its role in restoring electrophysiological alterations recorded via VEPs.

Acknowledgment

This study was supported by a Grant (No.: 2006.02.0122.013) from Akdeniz University Research Foundation.

References

Akpinar, D., Yargicoglu, P., Derin, N., Aslan, M., Agar, A., 2007. Effect of aminoguanidine on visual evoked potentials (VEPs), antioxidant status and lipid peroxidation in rats exposed to chronic restraint stress. Brain Res. 1186, 87–94.

Aslan, M., Cort, A., Yucel, I., 2008. Oxidative and nitrative stress markers in glaucoma. Free Radic. Biol. Med. 45, 367–376.

Aslan, M., Yucel, I., Ciftcioglu, A., Savaş, B., Akar, Y., Yucel, G., Sanlioglu, S., 2007. Corneal protein nitration in experimental uveitis. Exp. Biol. Med. (Maywood) 232, 1308–1313.

Aslan, M., Yücel, I., Akar, Y., Yücel, G., Ciftçioğlu, M.A., Sanlioglu, S., 2006. Nitrotyrosine formation and apoptosis in rat models of ocular injury. Free Radic Res. 40, 147–153.

Bazan, N.G., Marcheselli, V.L., Cole-Edwards, K., 2005. Brain response to injury and neurodegeneration: endogenous neuroprotective signaling. Ann. NY Acad. Sci. 1053, 137–147.

Cabrera, C.L., Wagner, L.A., Schork, M.A., Bohr, D.F., Cohan, B.E., 1999. Intraocular pressure measurement in the conscious rat. Acta Ophthalmol. Scand. 77, 33–36.

Clark, R.M., Yao, L., She, L., Furr, H.C., 2000. A comparison of lycopene and astaxanthin absorption from corn oil and olive oil emulsions. Lipids 35, 803–806.

Curek, G.D., Cort, A., Yucel, G., Demir, N., Ozturk, S., Elpek, G.O., Savas, B., Aslan, M., 2010. Effect of astaxanthin on hepatocellular injury following ischemia/reperfusion. Toxicology 267, 147–153.

Coleman, A.L., 1999. Glaucoma. Lancet 354, 1803–1810.

De La Paz, M.A., Epstein, D.L., 1996. Effect of age on superoxide dismutase activity of human trabecular meshwork. Invest. Ophthalmol. Vis. Sci. 37, 1849–1853.

Derin, N., Akpinar, D., Yargicoglu, P., Agar, A., Aslan, M., 2009. Effect of alpha-lipoic acid on visual evoked potentials in rats exposed to sulfite. Neurotoxicol. Teratol. 31, 34–39.

Fechtner, R.D., Weinreb, R.N., 1994. Mechanisms of optic nerve damage in primary open angle glaucoma. Surv. Ophthalmol. 39, 23–42.

Gaasterland, D., Tanishima, T., Kuwabara, T., 1978. Axoplasmic flow during chronic experimental glaucoma. 1. Light and electron microscopic studies of the monkey optic nervehead during development of glaucomatous cupping. Invest. Ophthalmol. Vis. Sci. 17, 838–846.

Gherghel, D., Griffiths, H.R., Hilton, E.J., Cunliffe, I.A., Hosking, S.L., 2005. Systemic reduction in glutathione levels occurs in patients with primary open-angle glaucoma. Invest. Ophthalmol. Vis. Sci. 46, 877–883.

Gottanka, J., Johnson, D.H., Martus, P., Lütjen-Drecoll, E., 1997. Severity of optic nerve damage in eyes with POAG is correlated with changes in the trabecular meshwork. J. Glaucoma. 6, 123–132.

Graham, S.L., Klistorner, A., 1998. Electrophysiology: a review of signal origins and applications to investigating glaucoma. Aust. NZ J. Ophthalmol. 26, 71–85.

Hall, A., Karplus, P.A., Poole, L.B., 2009. Typical 2-Cys peroxiredoxins – structures, mechanisms and functions. FEBS J. 276, 2469–2477.

Herr, D.W., King, D., Barone Jr., S., Crofton, K.M., 1995. Alterations in flash evoked potentials (FEPs) in rats produced by 3,3′-iminodipropionitrile (IDPN). Neurotoxicol. Teratol. 17, 645–656.

Howe, J.W., Mitchell, K.W., 1986. Visual evoked potential changes in chronic glaucoma and ocular hypertension. Trans. Ophthalmol. Soc. UK 105 (Pt 4), 457–462.

Ishida, K., Yamamoto, T., Kitazawa, Y., 1998. Clinical factors associated with progression of normal-tension glaucoma. J. Glaucoma. 7, 372–377.

Izzotti, A., 2003. DNA damage and alterations of gene expression in chronic-degenerative diseases. Acta Biochim. Pol. 50, 145–154.

JECFA, 1996. Toxicological evaluation of certain food additives and contaminants in food, WHO Food Additive Series, vol. 35, World Health Organization, Geneva.

Jewell, C., O'Brien, N.M., 1999. Effect of dietary supplementation with carotenoids on xenobiotic metabolizing enzymes in the liver, lung, kidney and small intestine of the rat. Br. J. Nutr. 81, 235–242.

Jia, L., Cepurna, W.O., Johnson, E.C., Morrison, J.C., 2000. Effect of general anesthetics on IOP in rats with experimental aqueous outflow obstruction. Invest. Ophthalmol. Vis. Sci. 41, 3415–3419.

Johnson, E.J., 2002. The role of carotenoids in human health. Nutr. Clin. Care. 5, 56–65.

Jonas, J.B., Budde, W.M., Lang, P., 1998. Neuroretinal rim width ratios in morphological glaucoma diagnosis. Br. J. Ophthalmol. 82, 1366–1371.

Kang, J.H., Pasquale, L.R., Willett, W., Rosner, B., Egan, K.M., Faberowski, N., Hankinson, S.E., 2003. Antioxidant intake and primary open-angle glaucoma: a prospective study. Am. J. Epidemiol. 158, 337–346.

Ko, M.L., Peng, P.H., Ma, M.C., Ritch, R., Chen, C.F., 2005. Dynamic changes in reactive oxygen species and antioxidant levels in retinas in experimental glaucoma. Free Radic. Biol. Med. 39, 365–373.

Krinsky, N.I., Johnson, E.J., 2005. Carotenoid actions and their relation to health and disease. Mol. Aspects Med. 26, 459–516.

Krinsky, N.I., Landrum, J.T., Bone, R.A., 2003. Biologic mechanisms of the protective role of lutein and zeaxanthin in the eye. Annu. Rev. Nutr. 23, 171–201.

Kurashige, M., Okimasu, E., Inoue, M., Utsumi, K., 1990. Inhibition of oxidative injury of biological membranes by astaxanthin. Physiol. Chem. Phys. Med. NMR 22, 27–38.

Landrum, J.T., Bone, R.A., Moore, L.L., Gomez, C.M., 1999. Analysis of zeaxanthin distribution within individual human retinas. Methods Enzymol. 299, 457–467.

Lehman, D.M., Harrison, J.M., 2002. Flash visual evoked potentials in the hypomyelinated mutant mouse shiverer. Doc. Ophthalmol. 104, 83–95.

Liu, B., Neufeld, A.H., 2000. Expression of nitric oxide synthase-2 (NOS-2) in reactive astrocytes of the human glaucomatous optic nerve head. Glia 30, 178–186.

Miyamoto, N., Izumi, H., Miyamoto, R., Kubota, T., Tawara, A., Sasaguri, Y., Kohno, K., 2009. Nipradilol and timolol induce Foxo3a and peroxiredoxin 2 expression and protect trabecular meshwork cells from oxidative stress. Invest. Ophthalmol. Vis. Sci. 50, 2777–2784.

Naguib, Y.M., 2000. Antioxidant activities of astaxanthin and related carotenoids. J. Agric. Food. Chem. 48, 1150–1154.

Nakajima, Y., Inokuchi, Y., Shimazawa, M., Otsubo, K., Ishibashi, T., Hara, H., 2008. Astaxanthin, a dietary carotenoid, protects retinal cells against oxidative stress in-vitro and in mice in-vivo. J. Phar. Pharmacol. 60, 1365–1374.

Nemesure, B., Wu, S.Y., Hennis, A., Leske, M.C., Barbados Eye Studies Group, 2003. Factors related to the 4-year risk of high intraocular pressure: the Barbados Eye Studies. Arch. Ophthalmol. 121, 856–862.

Neufeld, A.H., Sawada, A., Becker, B., 1999. Inhibition of nitric-oxide synthase 2 by aminoguanidine provides neuroprotection of retinal ganglion cells in a rat model of chronic glaucoma. Proc. Natl. Acad. Sci. USA 96, 9944–9948.

Nieminen, T., Lehtimäki, T., Mäenpää, J., Ropo, A., Uusitalo, H., Kähönen, M., 2007. Ophthalmic timolol: plasma concentration and systemic cardiopulmonary effects. Scand. J. Clin. Lab. Invest. 67, 237–245.

Ohgami, K., Shiratori, K., Kotake, S., Nishida, T., Mizuki, N., Yazawa, K., Ohno, S., 2003. Effects of astaxanthin on lipopolysaccharide-induced inflammation in vitro and in vivo. Invest. Ophthalmol. Vis. Sci. 44, 2694–2701.

Palozza, P., Krinsky, N.I., 1992. Astaxanthin and canthaxanthin are potent antioxidants in a membrane model. Arch. Biochem. Biophys. 297, 291–295.

Petri, D., Lundebye, A.K., 2007. Tissue distribution of astaxanthin in rats following exposure to graded levels in the feed. Comp. Biochem. Physiol. C Toxicol. Pharmacol. 145, 202–209.

Quigley, H.A., 1996. Number of people with glaucoma worldwide. Br. J. Ophthalmol. 80, 389–393.

Quigley, H.A., Addicks, E.M., 1980. Chronic experimental glaucoma in primates. II. Effect of extended intraocular pressure elevation on optic nerve head and axonal transport. Invest. Ophthalmol. Vis. Sci. 19, 137–152.

Roberts, R.L., Green, J., Lewis, B., 2009. Lutein and zeaxanthin in eye and skin health. Clin. Dermatol. 27, 195–201.

Reznick, A.Z., Packer, L., 1994. Oxidative damage to proteins: spectrophotometric method for carbonyl assay. Methods Enzymol. 233, 357–363.

Saccà, S.C., Izzotti, A., Rossi, P., Traverso, C., 2007. Glaucomatous outflow pathway and oxidative stress. Exp. Eye Res. 84, 389–399.

Saccà, S.C., Pascotto, A., Camicione, P., Capris, P., Izzotti, A., 2005. Oxidative DNA damage in the human trabecular meshwork: clinical correlation in patients with primary open-angle glaucoma. Arch. Ophthalmol. 123, 458–463.

Salmon, J.F., Glaucoma. Riordan-Eva, P., Whitcher, J.P., Asbury, T. (Eds.), 2008. Vaughan & Asbury's General Ophthalmology, 17th ed. (Chapter 11). McGraw-Hill, New York, pp. p212–p222.

Sawada, A., Neufeld, A.H., 1999. Confirmation of the rat model of chronic, moderately elevated intraocular pressure. Exp. Eye Res. 69, 525–531.

Schroeder, C.E., Tenke, C.E., Givre, S.J., Arezzo, J.C., Vaughan Jr, H.G., 1991. Striate cortical contribution to the surface-recorded pattern-reversal VEP in the alert monkey. Vision Res. 31, 1143–1157.

Shacter, E., 2000. Protein oxidative damage. Methods Enzymol. 319, 428–436.

Shareef, S., Sawada, A., Neufeld, A.H., 1999. Isoforms of nitric oxide synthase in the optic nerves of rat eyes with chronic moderately elevated intraocular pressure. Invest. Ophthalmol. Vis. Sci. 40, 2884–2891.

Shareef, S.R., Garcia-Valenzuela, E., Salierno, A., Walsh, J., Sharma, S.C., 1995. Chronic ocular hypertension following episcleral venous occlusion in rats. Exp. Eye Res. 61, 379–382.

Shibata, A., Kiba, Y., Akati, N., Fukuzawa, K., Terada, H., 2001. Molecular characteristics of astaxanthin and beta-carotene in the phospholipid monolayer and their distributions in the phospholipid bilayer. Chem. Phys. Lipids 113, 11–22.

Silver, S., Sohmer, H., Kapitulnik, J., 1995. Visual evoked potential abnormalities in jaundiced Gunn rats treated with sulfadimethoxine. Pediatr. Res. 38, 258–261.

Stadtman, E.R., Oliver, C.N., 1991. Metal-catalyzed oxidation of proteins. Physiological consequences. J. Biol. Chem. 266, 2005–2008.

Stahl, W., Sies, H., 2005. Bioactivity and protective effects of natural carotenoids. Biochim. Biophys. Acta 1740, 101–107.
Sucher, N.J., Lipton, S.A., Dreyer, E.B., 1997. Molecular basis of glutamate toxicity in retinal ganglion cells. Vision Res. 37, 3483–3493.
Tezel, G., 2006. Oxidative stress in glaucomatous neurodegeneration: mechanisms and consequences. Prog. Retin. Eye Res. 25, 490–513.
Tezel, G., Yang, X., 2004. Caspase-independent component of retinal ganglion cell death. Invest. Ophthalmol. Vis. Sci. 45, 4049–4059.
Tezel, G., Yang, X., Cai, J., 2005. Proteomic identification of oxidatively modified retinal proteins in a chronic pressure-induced rat model of glaucoma. Invest. Ophthalmol. Vis. Sci. 46, 3177–3187.
Towle, V.L., Moskowitz, A., Sokol, S., Schwartz, B., 1983. The visual evoked potential in glaucoma and ocular hypertension: effects of check size, field size, and stimulation rate. Invest. Ophthalmol. Vis. Sci. 24, 175–183.
Tso, M.O.M., Lam, T.T., 1996. Method of Retarding and Ameliorating Central Nervous System and Eye Damage. U.S. Patent #5527533.
Wasowicz, W., Nève, J., Peretz, A., 1993. Optimized steps in fluorometric determination of thiobarbituric acid-reactive substances in serum: importance of extraction pH and influence of sample preservation and storage. Clin. Chem. 39, 2522–2526.
Yan, D.B., Coloma, F.M., Metheetrairut, A., Trope, G.E., Heathcote, J.G., Ethier, C.R., 1994. Deformation of the lamina cribrosa by elevated intraocular pressure. Br. J. Ophthalmol. 78, 643–648.
Yücel, I., Akar, Y., Yücel, G., Ciftçioğlu, M.A., Keleş, N., Aslan, M., 2005. Effect of hypercholesterolemia on inducible nitric oxide synthase expression in a rat model of elevated intraocular pressure. Vision Res. 45, 1107–1114.
Yücel, I., Yücel, G., Akar, Y., Demir, N., Gürbüz, N., Aslan, M., 2006. Transmission electron microscopy and autofluorescence findings in the cornea of diabetic rats treated with aminoguanidine. Can. J. Ophthalmol. 41, 60–66.
Zhou, L., Li, Y., Yue, B.Y., 1999. Oxidative stress affects cytoskeletal structure and cell-matrix interactions in cells from an ocular tissue: the trabecular meshwork. J. Cell Physiol. 180, 182–189.